Formamidinium-Containing Metal-Halide: An Alternative Material for Near-IR Absorption Perovskite Solar Cells

ARTICLE *in* THE JOURNAL OF PHYSICAL CHEMISTRY C · JULY 2014

Impact Factor: 4.77 · DOI: 10.1021/jp411112k

9 AUTHORS, INCLUDING:

Teck Ming Koh
Nanyang Technological University
46 PUBLICATIONS **364** CITATIONS
SEE PROFILE

Shi Chen
Nanyang Technological University
66 PUBLICATIONS **1,468** CITATIONS
SEE PROFILE

Tze Chien Sum
Nanyang Technological University
142 PUBLICATIONS **3,378** CITATIONS
SEE PROFILE

Subodh G Mhaisalkar
Nanyang Technological University
383 PUBLICATIONS **8,188** CITATIONS
SEE PROFILE

THE JOURNAL OF PHYSICAL CHEMISTRY C

Article

pubs.acs.org/JPCC

Formamidinium-Containing Metal-Halide: An Alternative Material for Near-IR Absorption Perovskite Solar Cells

Teck Ming Koh,[†,⊥,‡] Kunwu Fu,[†,‡,⊥] Yanan Fang,[†,‡] Shi Chen,[§] T. C. Sum,[§] Nripan Mathews,[†,‡,∥] Subodh G. Mhaisalkar,[†,‡] Pablo P. Boix,*[,†] and Tom Baikie*[,†]

[†]Energy Research Institute @NTU (ERI@N), Research Techno Plaza, X-Frontier Block, Level 5, 50 Nanyang Drive, Singapore 637553

[‡]School of Materials Science and Engineering, Nanyang Technological University, Nanyang Avenue, Singapore 639798

[§]Division of Physics and Applied Physics, School of Physical and Mathematical Sciences, Nanyang Technological University, 21 Nanyang Link, Singapore, 637371

[∥]Singapore−Berkeley Research Initiative for Sustainable Energy, 1 Create Way, Singapore 138602, Singapore

Supporting Information

ABSTRACT: Solid-state, solution processed solar-cells based on organic−inorganic methyl ammonium lead halide absorbers have achieved efficiencies in excess of 15%, which has superseded liquid dye sensitized cells, as well as various thin film-based photovoltaics. This report introduces a new metal-halide perovskite, based on the formamidinium cation ($HC(NH_2)_2^+$), that displays a favorable band gap (1.47 eV) and represents a broader absorption compared to previously reported absorbers that contained the methylammonium cation ($CH_3NH_3^+$). The high open-circuit voltage (V_{oc} = 0.97 V) and promising fill-factor (FF = 68.7%) yield an efficiency of 4.3%, which make this material an excellent candidate for this new class of perovskite solar cell. This report also investigates the formation of a black trigonal ($P3m1$) perovskite polymorph and a yellow hexagonal nonperovskite ($P63mc$) polymorph. Further solar cell development would entail the stabilization of the black trigonal ($P3m1$) perovskite polymorph over the yellow hexagonal nonperovskite ($P63mc$) polymorph.

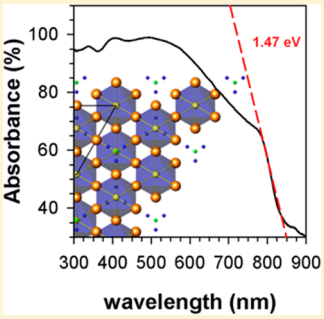

INTRODUCTION

Since the initial reports of solid-state solar cells based on organic−inorganic perovskite absorbers[1,2] [$CH_3NH_3PbX_3$ (X = I, Br, Cl)], such materials have attracted the attention of the photovoltaic community. Record power conversion efficiencies (PCE) of up to 15%[3,4] have been achieved and have placed this technology as a leading candidate for low cost solar energy production.

Although hybrid perovskites have been widely investigated for their photoactive properties,[5,6] the recent reports of $CH_3NH_3PbI_3$ containing solar cell devices have focused both on fabrication procedures (single step,[2] sequential deposition[3,7] and vapor deposition[4]) and different device architectures (planar[8] vs mesostructured[9,10]). This has led to some scrutiny about the role played by the $CH_3NH_3PbI_3$ perovskite layer, which has been shown to exhibit both electron and hole transporting behavior.[1,11] The high efficiencies of devices containing $CH_3NH_3PbI_3$ can be traced to its high absorption coefficient, good electrical transport properties, and favorable band gap (1.55 eV), which is close to the optimum value for a single junction solar cell.[12,13] However, the chemical modification of the X site anions (e.g., substitution of I for Br) has been achieved and was shown to increase the band gap while modulating the power conversion efficiencies (PCE).[14,15] Similarly, the substitution of the organic cation ($CH_3NH_3^+$) with a longer chain alkyl group ($C_2H_5NH_3^+$) was reported and resulted in a larger band gap and a lower power conversion efficiency (PCE) (2.4%).[16] Thus there is a need to explore alternative perovskites that have attractive band-gaps and can be formed into efficient solar cells. In this work we have investigated the use of the new absorber $HC(NH_2)_2PbI_3$, which contains the formamidinium cation [$HC(NH_2)_2^+$ = FA] in replacement of methylammonium cation (MA = $CH_3NH_3^+$) in the 'A' site of the perovskite structure, i.e., ABX_3. The FA cation has previously been shown to have a slightly larger ionic radius than the methylammonium group,[17,18] which is expected to lead to in an increase in perovskite tolerance factor (t),

$$t = \frac{r_A + r_X}{\sqrt{2}(r_B + r_X)}$$

where r_A, r_B, and r_X are the respective ionic radii of the ABX_3 ions in the perovskite structure. An increase in t while maintaining the ABX_3 perovskite structure generally leads to an increase in symmetry, with an expected reduction in electronic band gap (E_g = 1.47 eV). This band gap for $FAPbI_3$ is closer to the optimum value of ∼1.4 eV and presents $FAPbI_3$ as an

Special Issue: Michael Grätzel Festschrift

Received: November 12, 2013
Revised: December 13, 2013
Published: December 13, 2013

   dx.doi.org/10.1021/jp411112k | J. Phys. Chem. C 2014, 118, 16458−16462

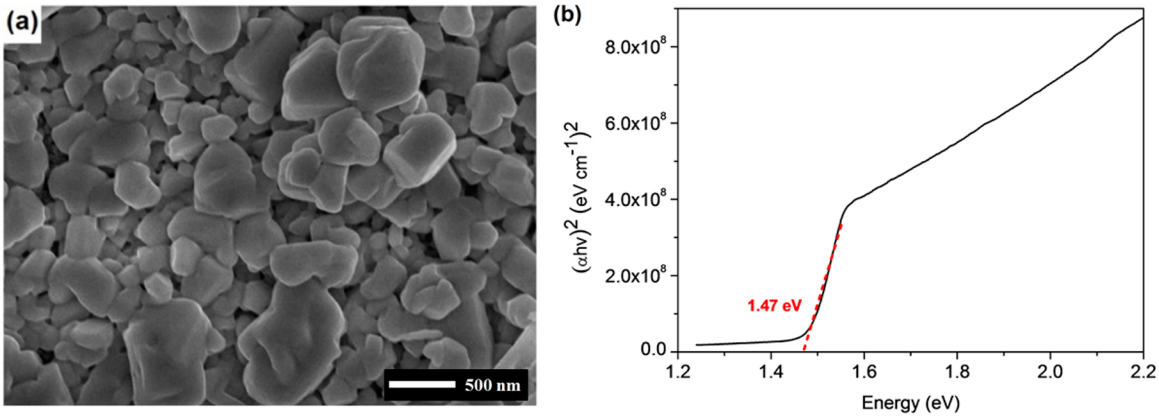

Figure 1. (a) Top view FESEM image and (b) Tauc plot of $FAPbI_3$ perovskite deposited on quartz substrate showing a band gap of 1.47 eV.

appealing candidate for photovoltaic applications, as it displays an extended absorption of light compared to the $MAPbI_3$ analogue.[19]

Herein, we report the synthesis and characterization of *FA*PbI_3 thin-films, with a focus on the key requirements for photovoltaic applications such as band gap, energetics and absorption, as well as an effective route to a mesoscopic solution processed solar cell devices. Our best performing device displayed a power conversion efficiency (PCE) greater than 4%, and it is, to the best of our knowledge, the first photovoltaic device containing $FAPbI_3$. While the present study highlights the structural instability of the photoactive black polymorph of $FAPbI_3$, it is believed that through appropriate control and optimization of the synthetic procedures for the stabilization of this material, PCE comparable to that of $CH_3NH_3PbI_3$ can be achieved.

EXPERIMENTAL DETAILS

Synthesis of Formamidinium Iodide [$HC(NH_2)_2I$]. The [$HC(NH_2)_2I$] was synthesized using a modified literature method.[19] A 1 equivalent formamidine hydrochloride (Sigma Aldrich) methanol solution was added to a 1 equiv solution sodium hydroxide in methanol. The solution was allowed to stir for 1 h, and the precipitate was discarded. The solution was then dried using a rotary evaporator and the solid was redissolved in ethanol. HI (1.2 equiv; Sigma Aldrich, 57 wt % in H_2O) was then added, and the solution and stirred for 2 h. The solution was then dried again using a rotary evaporator and the solid obtained was washed thoroughly using ether until a white crystalline solid was obtained. Yield: 79%.

^1H NMR (400 MHz, DMSO-d_6): δ 8.49 (s, 4H), 7.8 (s, 1H). ^{13}C NMR (400 MHz, DMSO-d_6): δ 158.1.

Device Fabrication. The detailed device fabrication process is as follows: Fluorine doped tin oxide (FTO) glass was etched with zinc powder and diluted HCl solution. The etched substrates were cleaned by ultrasonication in decon-soap solution, deionized water and ethanol, respectively, and then subjected to an O_3/UV treatment. A compact layer of TiO_2 was deposited onto the FTO surface by spray pyrolysis process with titanium diisopropoxide bis(acetylacetonate) solution (75% in 2-propanol,Sigma-Aldrich) diluted in ethanol (1:9 v/v). After cooling to room temperature, the substrates were treated in a 0.04 M $TiCl_4$ solution for 30 min at 70 °C. Mesoporous TiO_2 (mp-TiO_2) film was spin-coated onto the FTO surface with DYESOL-30NRD paste, that was diluted with ethanol with a ratio of 1:5 w/w, and sintered at 500 °C for 30 min. The films were then treated with 40 mM $TiCl_4$ solution at 70 °C for 30 min and heated at 500 °C again for 30 min. When cooled to room temperature, the PbI_2 solution was spin-coated onto the mesoporous film at 6000 rpm for 5s and then heated at 70 °C for 30 min. The films were then immersed into a $HC(NH_2)_2I$ solution with a concentration of 8 mg/mL for 15 min, after which they were rinsed with IPA and spin-coated at 4000 rpm for 30 s.

2,2′,7,7′-tetrakis(*N*,*N*′-di-*p*-methoxyphenylamine)-9,9′-spirobifluorene (spiro-OMeTAD) was dissolved in chlorobenzene at 100 mg/mL, heated to 70 °C for 30 min. 15.92 μL *tert*-butylpyridine (TBP) and 9.68 μL lithium bis(trifluoromethylsulfonyl)imide (Li-TFSI, 520 mg/mL in acetonitrile) were added directly to the 300 μL solution. A total of 3.6 mg tris(2-(1*H*-pyrazol-1-yl)pyridine)cobalt(III) tris(hexafluorophosphate) Co-dopant (FK102) was predissolved into acetonitrile and added into the hole-transport material solution. The as-prepared solution was spin-coated onto the film at 4000 rpm for 30s. A 100 nm Au cathode layer was deposited by thermal evaporation with a 0.2 cm^2 metallic mask.

Characterization. Photovoltaic measurements utilized an AM 1.5G solar simulator equipped with a 450 W xenon lamp (model 81172, Oriel). Its power output was adjusted to match AM 1.5G sunlight (100 mW/cm^2) by using a reference Si photodiode. *I*−*V* curves were obtained by applying an external bias to the cell and measuring the generated photocurrent with a Keithley model 2612A digital source meter. All devices were measured by masking the active area with a black tape mask. Incident-photon-to-current conversion efficiency (IPCE) was measured using a PVE300 (Bentham), with a dual Xenon/quartz halogen light source, measured in DC mode, and no bias light was used. The absorption spectra of the spin-coated $HC(NH_2)_2PbI_3$ films were measured using a UV−vis spectrometer (SHIMADZU, UV-3600 UV−vis−NIR Spectrophotometer) with an integrated sphere (ISR-3100). ^1H and ^{13}C NMR data were obtained on a Bruker DPX 400 MHz spectrometer with chemical shifts referenced to DMSO-d_6

The morphology features of the perovskite-coated and PbI_2-coated mesoporous TiO_2 films were observed with a field-emission scanning electron microscopy (FE-SEM, JEOL JSM 6700F). Sample purity was established using powder X-ray diffraction. Data were collected using a Bruker D8 Advance diffractometer fitted with a CuK_α source operated at 40 kV and 40 mA, a 1° divergence slit, 0.3 mm receiving slit, a secondary graphite monochromator, and a Lynxeye silicon strip detector.

dx.doi.org/10.1021/jp411112k | *J. Phys. Chem. C* 2014, 118, 16458−16462

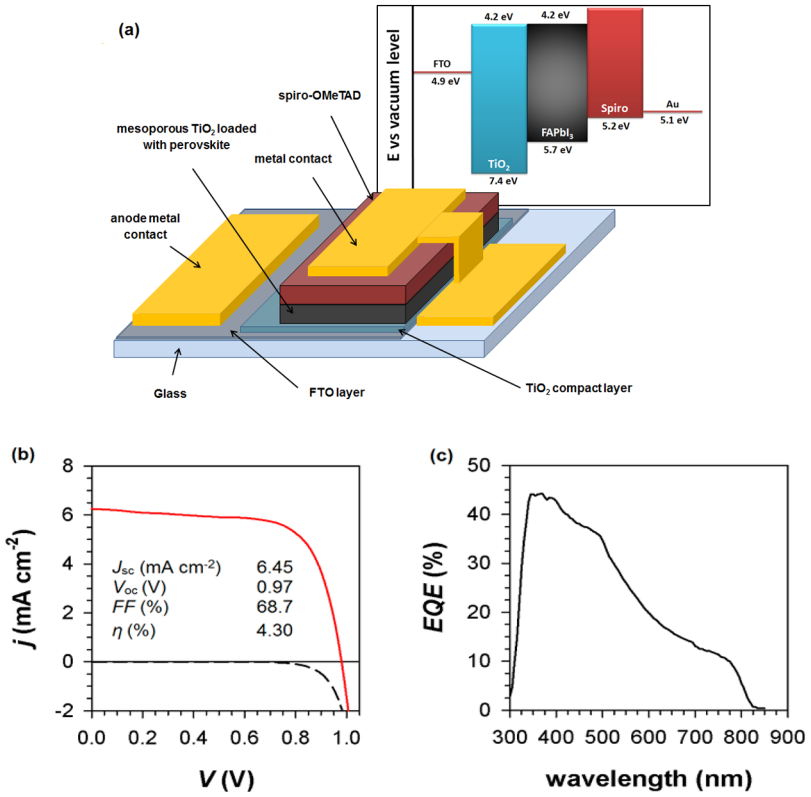

Figure 2. (a) Device structure of the solar cell. In the inset, energy level diagram for the reported $FAPbI_3$-based solar cell. The band gap and valence band maximum values of the absorber were calculated from the UV–vis absorption and UPS measurements. (b) Current–voltage curve for the $FAPbI_3$ device under AM1.5G illumination and dark conditions. (c) EQE (external quantum efficiency) of the solar cell.

A thin-film of the perovskite was deposited on a glass slide and heated at 150 °C for 60 min before data collection. Data were accumulated from 10° to 70° 2θ using a step size of 0.02° with a dwell time of 0.2s per step. Pawley fits of the diffraction data were performed using TOPAS V4.1 using a pseudo-Voigt peak shape function in combination with the reported cell data for the different polymorphs of $FAPbI_3$[19] and the 2*H* polymorph of PbI_2.

The XPS and UPS are measured in a homemade UHV system with the base pressure at 3×10^{-10} Torr. A hemispheric electron analyzer (Omicron, EA125) is used to detect the photoelectron excited by a monochromatic Al Kα radiation ($h\nu$ = 1486.7 eV) or UV light (He I, $h\nu$ = 21.2 eV).

RESULTS AND DISCUSSION

PbI_2 was first spin-coated on the TiO_2 mesoporous layer, and following the sequential deposition process,[3,7,9] the films were then immersed into a $HC(NH_2)_2I$ solution for conversion to $FAPbI_3$. SEM image shown in Figure 1a indicates the presence of perovskite crystals on top of the film. For comparison, an SEM image of a TiO_2/PbI_2 film prior to the conversion is provided in the Supporting Information (see Figure S1). The treated film highlights the formation of *FA*PbI_3 in crystals ranging from hundreds of nanometers to micrometers in size.

The optical absorption measurements shown in Figure 1b indicate a band gap of ~1.47 eV, which is in good agreement with previous reports[19] and lower than that of $CH_3NH_3PbI_3$.[20] Additionally, ultraviolet photoelectron spectroscopy (UPS) measurements (see Figure S2 in Supporting Information) confirmed the suitable energetics for hole injection into spiro-OMeTAD (Figure 2a). It is worth remarking that the value obtained for the conduction band of the perovskite is in the same range as that generally reported for TiO_2. Although the positioning of the perovskite band could hinder the electron injection into TiO_2, the inherent energetic disorder of the TiO_2 broadens the shape of its conduction band, which should contribute to enabling the injection process.[19]

When the films were implemented in the solar cells (Figure 2a), the fabricated devices exhibited an encouraging performance of 4.3%, a remarkably high open-circuit potential close to 1 V (V_{oc} = 0.97 V) and a fill factor (FF) of 68.7% (Figure 2b). These values are in the range of those found in the best performing photovoltaic efficiencies obtained for perovskite devices containing $CH_3NH_3PbI_3$, except for the short circuit current density (J_{sc} = 6.45 mA cm^{-2}), which showed a much lower value. The EQE onset wavelength (Figure 2c), in good agreement with the absorption spectra, shows an extended absorption of the light, and to the best of our knowledge, is the broadest one obtained for an organic–inorganic halide perovskites.[14]

However, the low value of EQE limits the device photocurrent and could be partially due to the energetic mismatch of TiO_2 and perovskite conduction bands. Additionally, $FAPbI_3$ reportedly exists as two polymorphs: a black perovskite-type material with trigonal symmetry ($P3m1$), and a yellow hexagonal nonperovskite counterpart ($P6_3mc$).[19] In order to elucidate the latter effect in more detail, samples of *FA*PbI_3 were sequentially deposited on glass substrates and analyzed using powder X-ray diffraction (PXRD) (Figure 3a). Using the reported space group and lattice parameters for the $FAPbI_3$ perovskite, a Pawley fit was carried out with the PXRD data and the extracted lattice parameters (a = 8.9920(9) c = 11.0139(7)

dx.doi.org/10.1021/jp411112k | J. Phys. Chem. C 2014, 118, 16458–16462

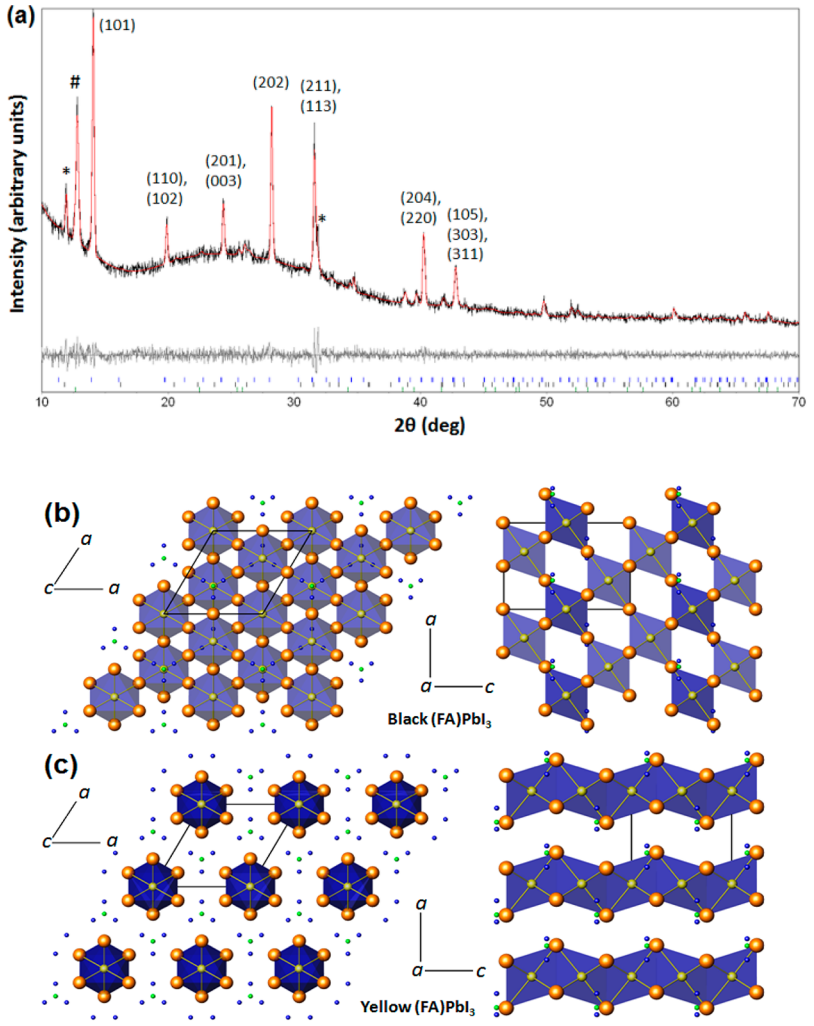

Figure 3. (a) A Pawley fit of the powder X-ray diffraction of pattern for $FAPbI_3$ perovskite thin film prepared via a sequential deposition process. The reflections indicated by * and # represent the Bragg reflections associated with the yellow polymorph of $FAPbI_3$ and PbI_2, respectively. The indexed reflections associated with the black perovksite polymorph are indicated in the plot. Polyhedral representations of the black (b) and yellow (c) polymorphs of $FAPbI_3$. The blue polyhedra represent the PbI_6 octahedra with the Pb and I atoms shown as yellow and orange spheres respectively. Both structures are shown viewed along the crystallographic *c* (left) and *a* (right) axes, respectively. In the black polymorph the inorganic component consists of a three-dimensional network of corner linked PbI_6 octahedra with the yellow polymorph containing linear chains of face-sharing octahedra. The N and C ions of the formamidimium cations are shown as blue and green spheres, respectively.

Å) are in good agreement with the reported values (a = 8.9817(13) Å c = 11.006(2) Å)[19] for the desired perovskite phase (represented in Figure 3b). However, the XRD patterns typically showed the coexistence of the yellow polymorph of $FAPbI_3$ (in Figure 3c) as well as the 2*H*-polymorph of PbI_2.[19] The apparent larger band gap of the yellow $FAPbI_3$ polymorph together with its chain-like structure that is likely to hinder electron transport through the material is possibly another reason for a reduction in the photovoltaic performance, particularly reducing the value of the EQE spectrum.

Previous work[19] found that the black perovskite-type polymorph was the most favorable at T > 60 °C with the yellow polymorph favored at lower temperatures. However, it was reported that if the black phase was separated from the mother liquor at T > 60 °C and then dried, it was sufficiently stable to remain in the perovskite structure when cooled to room temperature. Although the interconversion was reportedly slowed down rather than halted, the black material was apparently stable in dry air for weeks but lost its crystalline luster quickly in a humid atmosphere. A general trend observed is that methyl-ammonium-containing materials are considerably more stable than formamidinium-containing ones.

In an ambient humid atmosphere the black perovskite films were observed to turn yellow in color with PXRD revealing an increase of the Bragg reflections consistent with the hexagonal yellow polymorph of $FAPbI_3$ (see Supporting Information). Interestingly, the powder XRD pattern of the ambient exposed samples showed an unusual texture effect for the perovskite where only the [101] planes were evident with the 202 reflection as the most intense. This effect was consistently observed in the thin films and warrants further investigation. However, when the films were implemented into the full solar cell device the films remained dark in color, which is attributed to a slightly improvement of the stability possibly due to a sealing effect of the spiro-OMeTAD. Further optimization of the synthesis and stabilization of the black phase will certainly lead to higher efficiency devices.

dx.doi.org/10.1021/jp411112k | *J. Phys. Chem. C* 2014, 118, 16458−16462

CONCLUSION

This work opens novel routes to achieve high efficiency perovskite solar cells as well as to develop alternative perovskite absorbers containing the FA cation. Absorption measurements displayed a bandgap of 1.47 eV for $FAPbI_3$. This extends the absorption toward longer wavelengths compared to previously reported perovskites containing the $CH_3NH_3^+$ group, a promising approach to increase the PCE. UPS measurements showed a favorable valence band for hole injection to the spiro-OMeTAD. However, the low values of the EQE are attributed to the low driving force for electron injection into TiO_2, as well as to the presence of a nonperovskite structured yellow polymorph of $FAPbI_3$. The aim of our future work will be focused on improving the synthetic process to enable the stabilization of the black perovskite polymorph, replacement of the Pb and I with suitable elements in their class to facilitate tuning of energy levels, and attempting the perovskite deposition on alternative mesoporous semiconductor than TiO_2.

ASSOCIATED CONTENT

Supporting Information

FESEM image and of PbI_2 deposited on mesoporous TiO_2 film, UPS spectrum of $CH(NH_2)_2PbI_3$ thin film on FTO and powder X-ray diffraction pattern for yellow polymorph in $FAPbI_3$ perovskite thin film. This information is available free of charge via the Internet at http://pubs.acs.org.

AUTHOR INFORMATION

Corresponding Authors

*E-mail: PBPablo@ntu.edu.sg; Tel: +65 9723 9775 (P.P.B.).
*E-mail: TBaikie@ntu.edu.sg; Tel: +65 8164 6442 (T.B.).

Author Contributions

⊥These authors contributed equally in this work.

Notes

The authors declare no competing financial interest.

ACKNOWLEDGMENTS

This work was supported by the National Research Foundation (NRF), Singapore, under the Competitive Research Program (NRF-CRP4-2008-03) and the SinBeRISE CREATE program. The authors would like to thank Dr. Herlina Arianita Dewi for her contribution in the SEM imaging and Mr. Lim Swee Sien for photoluminescence measurements.

REFERENCES

(1) Lee, M. M. M.; Teuscher, J.; Miyasaka, T.; Murakami, T. N.; Snaith, H. J.; Henry, J. Efficient Hybrid Solar Cells Based on Meso-Superstructured Organometal Halide Perovskites. *Science* **2012**, *338*, 643−647.

(2) Kim, H.-S.; Lee, C.-R.; Im, J.-H.; Lee, K.-B.; Moehl, T.; Marchioro, A.; Moon, S.-J.; Humphry-Baker, R.; Yum, J.-H.; Moser, J. E.; et al. Lead Iodide Perovskite Sensitized All-Solid-State Submicron Thin Film Mesoscopic Solar Cell with Efficiency Exceeding 9%. *Sci. Rep.* **2012**, *2*, 591.

(3) Burschka, J.; Pellet, N.; Moon, S.-J.; Humphry-Baker, R.; Gao, P.; Nazeeruddin, M. K.; Grätzel, M. Sequential Deposition as a Route to High-Performance Perovskite-Sensitized Solar Cells. *Nature* **2013**, *499*, 316−319.

(4) Liu, M.; Johnston, M. B.; Snaith, H. J. Efficient Planar Heterojunction Perovskite Solar Cells by Vapour Deposition. *Nature* **2013**, *501*, 395−398.

(5) Mitzi, D. B.; Wang, S.; Feild, C. A.; Chess, C. A.; Guloy, A. M. Conducting Layered Organic-Inorganic Halides Containing ⟨110⟩-Oriented Perovskite Sheets. *Science* **1995**, *267*, 1473−1476.

(6) Mitzi, D. B.; Feild, C. A.; Harrison, W. T. A. Conducting Tin Halides with a Layered Organic-Based Perovskite Structure. *Nature* **1994**, *369*, 467−469.

(7) Liang, K.; Mitzi, D. B.; Prikas, M. T. Synthesis and Characterization of Organic−Inorganic Perovskite Thin Films Prepared Using a Versatile Two-Step Dipping Technique. *Chem. Mater.* **1998**, *4756*, 403−411.

(8) Eperon, G. E.; Burlakov, V. M.; Docampo, P.; Goriely, A.; Snaith, H. J. Morphological Control for High Performance, Solution-Processed Planar Heterojunction Perovskite Solar Cells. *Adv. Funct. Mater.* **2013**, DOI: 10.1002/adfm.201302090.

(9) Sabba, D.; Kumar, H. M.; Yantara, N.; Pham, T. T. T.; Park, N.-G.; Gratzel, M.; Mhaisalkar, S. G.; Mathews, N.; Boix, P. P. High Efficiency Electrospun TiO_2 Nanofiber Based Hybrid Organic−Inorganic Perovskite Solar Cell. *Nanoscale* **2013**, *49*, 11089−11091.

(10) Qiu, J.; Qiu, Y.; Yan, K.; Zhong, M.; Mu, C.; Yan, H.; Yang, S. All-Solid-State Hybrid Solar Cells Based on a New Organometal Halide Perovskite Sensitizer and One-Dimensional TiO_2 Nanowire Arrays. *Nanoscale* **2013**, *5*, 3245−3248.

(11) Etgar, L.; Gao, P.; Xue, Z.; Peng, Q.; Chandiran, A. K.; Liu, B.; Nazeeruddin, M. K.; Grätzel, M. Mesoscopic $CH_3NH_3PbI_3/TiO_2$ Heterojunction Solar Cells. *J. Am. Chem. Soc.* **2012**, *134*, 17396−17399.

(12) Xing, G.; Mathews, N.; Sun, S.; Lim, S. S.; Lam, Y. M.; Gratzel, M.; Mhaisalkar, S.; Sum, T. C. Long-Range Balanced Electron- and Hole-Transport Lengths in Organic−Inorganic $CH_3NH_3PbI_3$. *Science* **2013**, *342*, 344−347.

(13) Stranks, S. D.; Eperon, G. E.; Grancini, G.; Menelaou, C.; Alcocer, M. J. P.; Leijtens, T.; Herz, L. M.; Petrozza, A.; Snaith, H. J. Electron-Hole Diffusion Lengths Exceeding 1 Micrometer in an Organometal Trihalide Perovskite Absorber. *Science* **2013**, *342*, 341−344.

(14) Noh, J. H.; Im, S. H.; Heo, J. H.; Mandal, T. N.; Seok, S. I. Chemical Management for Colorful, Efficient, and Stable Inorganic-Organic Hybrid Nanostructured Solar Cells. *Nano Lett.* **2013**, *13*, 1764−1769.

(15) Edri, E.; Kirmayer, S.; Cahen, D.; Hodes, G. High Open-Circuit Voltage Solar Cells Based on Organic−Inorganic Lead Bromide Perovskite. *J. Phys. Chem. Lett.* **2013**, *4*, 897−902.

(16) Im, J.-H.; Chung, J.; Kim, S.-J.; Park, N.-G. Synthesis, Structure, and Photovoltaic Property of a Nanocrystalline 2H Perovskite-type Novel Sensitizer $(CH_3CH_2NH_3)PbI_3$. *Nanoscale Res. Lett.* **2012**, *7*, 353.

(17) Mitzi, D. B.; Liang, K. Synthesis, Resistivity, and Thermal Properties of the Cubic Perovskite $NH_2CH{=}NH_2SnI_3$ and Related Systems. *J. Solid State Chem.* **1997**, *134*, 376−381.

(18) Knutson, J. L.; Martin, J. D.; Mitzi, D. B. Tuning the Band Gap in Hybrid Tin Iodide Perovskite Semiconductors Using Structural Templating. *Inorg. Chem.* **2005**, *44*, 4699−4705.

(19) Stoumpos, C. C.; Malliakas, C. D.; Kanatzidis, M. G. Semiconducting Tin and Lead Iodide Perovskites with Organic Cations: Phase Transitions, High Mobilities, and Near-Infrared Photoluminescent Properties. *Inorg. Chem.* **2013**, *52*, 9019−9038.

(20) Baikie, T.; Fang, Y. N.; Kadro, J. M.; Schreyer, M.; Wei, F. X.; Mhaisalkar, S. G.; Graetzel, M.; White, T. J. Synthesis and Crystal Chemistry of the Hybrid Perovskite $(CH_3NH_3)PbI_3$ for Solid-State Sensitised Solar Cell Applications. *J. Mater. Chem. A* **2013**, *1*, 5628−5641.